Development Engineering 5 (2020) 100049

Contents lists available at ScienceDirect

Development Engineering

journal homepage: http://www.elsevier.com/locate/deveng

Practical design considerations for secondary air injection in wood-burning cookstoves: An experimental study

Julien J. Caubel [a,b,*], Vi H. Rapp [b], Sharon S. Chen [b], Ashok J. Gadgil [b,c]

[a] Department of Mechanical Engineering, University of California, Berkeley, Berkeley, CA, 94720, United States
[b] Environmental Technologies Area, Lawrence Berkeley National Laboratory, Berkeley, CA, 94720, United States
[c] Department of Civil and Environmental Engineering, University of California, Berkeley, Berkeley, CA, 94720, United States

ARTICLE INFO

Keywords:
Biomass cookstove
Household energy
Air pollution
Design
Combustion

ABSTRACT

Billions of households worldwide cook using biomass fires and suffer from the toxic smoke emitted into their homes. Laboratory studies of wood-burning cookstoves demonstrate that secondary air injection can greatly reduce the emission of harmful air pollution, but these experimental advancements are not easily translated into practical cookstove designs that can be widely adopted. In this study, we use a modular cookstove platform to experimentally quantify the practical secondary air injection design requirements (e.g., flow rate, pressure, and temperature) to reduce mass emissions of particulate matter (PM), carbon monoxide (CO), and black carbon (BC) by at least 90% relative to a traditional cooking fire. Over the course of 111 experimental trials, we illuminate the physical mechanisms that drive emission reductions, and outline fundamental design principles to optimize cookstove performance. Using the experimental data, we demonstrate that low-cost (<$10) fans and blowers are available to drive the secondary flow, and can be independently powered using an inexpensive thermoelectric generator mounted nearby. Furthermore, size-resolved PM measurements show that secondary air injection inhibits particle growth, but the total number of particles generated remains relatively unaffected. We discuss the potential impacts for human health and investigate methods to mitigate the PM formation mechanisms that persist.

1. Introduction

Over 2 billion people cook using solid biomass fuels, such as wood and dung (Bonjour et al., 2013; Legros et al., 2009). Typically, households rely on traditional biomass cookstoves that are highly inefficient and polluting (Bruce et al., 2000; Malla and Timilsina, 2014). When these cookstoves are used in poorly ventilated homes, indoor concentrations of harmful pollutants, such as particulate matter (PM) and carbon monoxide (CO), can be up to 100 times higher than levels recommended by the World Health Organization (WHO) (Edwards et al., 2014; Smith et al., 2007; Chen et al., 2016a). As a result, chronic exposure to indoor air pollution from solid biomass cookstoves is a leading environmental health risk, causing nearly 2 million premature deaths annually (Stanaway et al., 2018; Foell et al., 2011).

Some biomass cookstoves are designed to reduce unwanted emissions by using a small fan or blower to inject secondary air into the combustion chamber (Jetter et al., 2012; Jetter and Ebersviller, 2015; Delapena et al., 2015; Still et al., 2015; Sutar et al., 2015). When properly injected, the jets of secondary air increase the turbulent mixing and residence time of gas-phase fuel in the combustion zone, while providing oxygen directly to fuel-rich regions (Lamberg et al., 2011; Lyngfelt and Leckner, 1999; Nuutinen et al., 2014; Okasha, 2007; Wiinikka and Gebart, 2004; Caubel et al., 2018; Rapp et al., 2016). As a result, fuel oxidation is more complete, fewer harmful pollutants are emitted, and thermal efficiency is enhanced (Sutar et al., 2015; Lamberg et al., 2011). However, secondary air is typically much cooler than the

Abbreviations: APS, Aerodynamic Particle Sizer; BC, Black Carbon; CAI, California Analytical Instruments; CO_2, Carbon Dioxide; CO, Carbon Monoxide; FMPS, Fast Mobility Particle Sizer; kWd, kilowatt of thermal power delivered to the cooking pot; LBNL, Lawrence Berkeley National Laboratory; MOD, Modular Air Injection Stove: Version 1; MOD2, Modular Air Injection Stove: Version 2; PAH, Polycyclic Aromatic Hydrocarbon; PM, Particulate Matter; $PM_{2.5}$, Particulate Matter with an aerodynamic diameter ≤2.5 μm; ppmv, parts per million by volume; TEG, Thermoelectric Generator; TSF, Three Stone Fire; UFP, Ultrafine Particle; US EPA, United States Environmental Protection Agency; WBT, Water Boiling Test; WHO, World Health Organization.

* Corresponding author. 1 Cyclotron Road, MS 90R2121, Berkeley, CA, 94720, United States.
E-mail address: jcaubel@berkeley.edu (J.J. Caubel).

https://doi.org/10.1016/j.deveng.2020.100049
Received 24 May 2019; Received in revised form 23 January 2020; Accepted 23 January 2020
Available online 4 February 2020

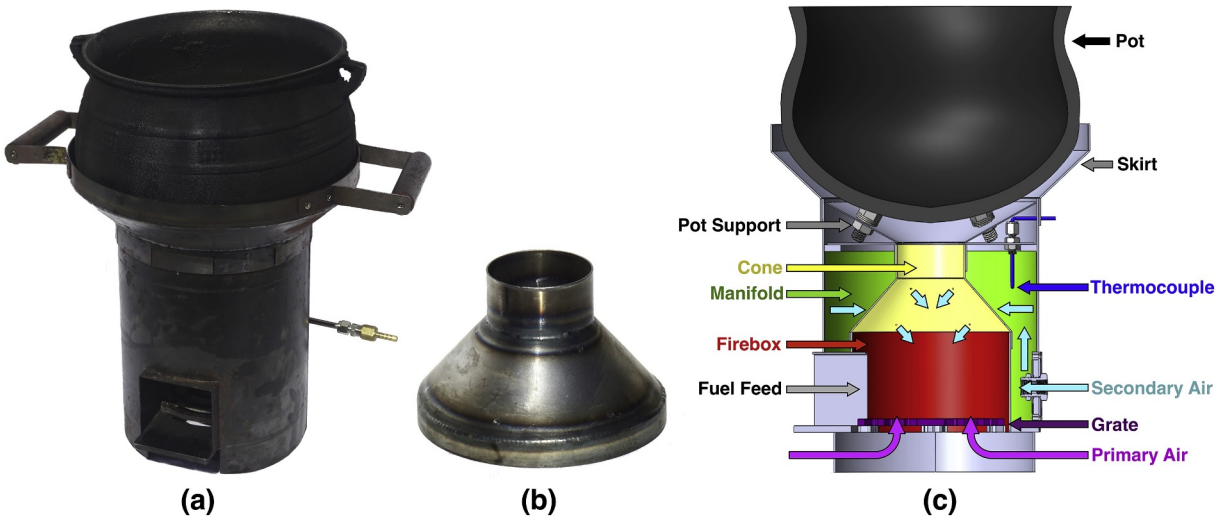

Fig. 1. (a) The MOD2 stove with cast-aluminum Darfuri pot; (b) Removable conical chimney, into which secondary air injection patterns are drilled; (c) Cross-sectional view of the MOD2 stove showing the firebox, conical chimney, secondary air manifold, secondary air flow path, and other design features. Air injection holes are enlarged (out of scale) for clarity.

exhaust gases and improper injection can result in lower combustion temperatures that limit fuel oxidation and heat transfer to the thermal load (e.g. a cooking pot) (Wiinikka and Gebart, 2004; Caubel et al., 2018; Rapp et al., 2016; Pettersson et al., 2010; Tryner et al., 2016). For example, Jetter et al. evaluated the performance of several secondary air injection cookstoves and showed that half do not reduce PM or CO mass emissions relative to a three stone fire (TSF) (Jetter et al., 2012).

Studies have shown that many secondary air injection design parameters, such as the flow rate and geometry, must be carefully considered and validated in order to significantly reduce unwanted emissions from biomass combustion appliances (Lamberg et al., 2011; Lyngfelt and Leckner, 1999; Wiinikka and Gebart, 2004; Caubel et al., 2018; Rapp et al., 2016; Tryner et al., 2016; Nussbaumer, 2003; Vicente and Alves, 2018). However, current studies do not usually consider the critical operational parameters needed to appropriately size the core components of a practical, stand-alone cookstove. For example, no information is provided on the positive pressure required to drive the secondary air injection flow, although this information is required to select fans or blowers. Consequently, emission reductions achieved in the laboratory are not easily translated into cookstove designs that can be manufactured, distributed, and adopted on a large scale.

In this study, we use an experimental cookstove platform to investigate the practical secondary air injection design requirements for reducing the mass emission of air pollutants from unprocessed wood combustion by one order of magnitude. We conducted 111 experimental trials, systematically varying critical secondary air injection parameters (e.g. flow rate and location) to identify a design configuration that emits 90% less CO, PM, and (BC) than a TSF, and also improves thermal efficiency. We targeted mass emission reductions of at least 90% because indoor pollution concentrations from traditional biomass cooking easily exceed health guidelines by 10 times or more (Bruce et al., 2000; Smith et al., 2007; Chen et al., 2016a; Soneja et al., 2015). Throughout the experimental optimization, we recorded the secondary air injection flow rate, pressure and temperature to evaluate whether the performance improvements are practically achievable using inexpensive, off-the-shelf components that can be powered independently (e.g., small fans powered by a thermoelectric generator). Furthermore, we use size-resolved PM measurements to investigate the underlying physical mechanisms contributing to the reduction of total PM mass emissions and identify particle size ranges where further emission reductions are needed.

2. Materials and methods

2.1. Modular air injection cookstove design: version 2 (MOD2)

The MOD2 stove, presented in Fig. 1, is a continuously fed, wood-burning cookstove that enables critical secondary air injection parameters to be modulated easily and repeatably. The MOD2 stove is the second design iteration of the modular (MOD) stove described by Caubel et al. (2018), and therefore shares the same general design architecture and accommodates the same cast-aluminum Darfuri cooking pot. The MOD2 stove has a cylindrical firebox, 15 cm (6 inch) in diameter, with an open fuel feed at the front. Primary air enters the firebox through the open fuel feed, and adjustable openings below the grate. Above the firebox, a conical chimney reduces to a 6.4-cm (2.5-inch) diameter throat located directly below the pot. An integrated air manifold surrounds the firebox and conical chimney assembly (Fig. 1(c)). Secondary air is supplied to a port at the back of the manifold and is injected into the firebox through orifices drilled into the conical chimney. The conical chimney is removable, such that different air injection patterns can easily be drilled, installed, and tested (Fig. 1(b)). The pot's height above the chimney throat is controlled using adjustable supports. The stove also incorporates a steel skirt that closely surrounds the pot to enhance the rate of heat transfer from the exhaust gases.

Previous research on the MOD stove (version 1) demonstrated that higher secondary air injection velocities improved stove performance, but excessive secondary flow quenched the combustion (Caubel et al., 2018). The velocity of the secondary air jets decreases rapidly after injection into the firebox. For the 1.59-mm (0.0625-inch) diameter secondary air injection orifices used throughout the MOD stove (version 1) study, the average jet velocity diminishes by 90% over a normal distance of just 4 cm (Lienhard and Lienhard, 1984; Cushman-Roisin, 2014), or less than half of the distance required to reach the center of the MOD stove's firebox. To ensure that secondary air jets better reach the flames, the MOD2 stove's firebox and conical chimney diameters are approximately 15% smaller than in the MOD stove. By reducing the distance from the orifices to the combustion zone, the velocity of the air jets is higher when they reach the flames, thereby promoting turbulent mixing and oxygen injection at lower secondary flow rates that do not prohibitively cool the combustion. MOD2 stove dimensions were not reduced further, as a 15-cm firebox was deemed to be the smallest size that allows easy feeding and tending of the firewood. Additional details regarding the MOD2 stove design are provided in the SI.

2.2. Experimental set-up and stove testing procedure

The MOD2 stove was developed at Lawrence Berkeley National Laboratory's (LBNL) cookstove testing facility. The experimental setup and testing procedure for the MOD2 stove are the same as that described by Caubel et al. for the MOD stove (version 1) (Caubel et al., 2018), and a brief overview is provided here. During testing, emissions from the MOD2 stove are completely captured using a steel hood, and exhausted outdoors using a steel ducting system and blowers. Air pollution instruments sample the duct flow and provide emission concentration measurements every second (1 Hz). A California Analytical Instruments 600 Series gas analyzer measures the volumetric concentrations (ppmv) of CO, carbon dioxide (CO_2), and oxygen (O_2). The total mass of $PM_{2.5}$ (PM with aerodynamic diameter $\leq$ 2.5 μm) emitted during the test phase is measured gravimetrically. A suite of real-time PM instruments sample emissions from the duct using a secondary diluter. A TSI 3091 Fast Mobility Particle Sizer (FMPS) and a TSI 3321 Aerodynamic Particle Sizer (APS) together provide size-resolved particle number concentration measurements from 5 to 2500 nm, while a Magee Scientific AE-22 Aethalometer provides black carbon (BC) mass concentration measurements. All instruments were calibrated according to manufacturer recommendations, as described by Caubel et al. (2018)

The MOD2 stove was tested using the cold start, high power phase of the Water Boiling Test (WBT) 4.2.3 as pollutant emissions are usually highest during this phase of stove use (Caubel et al., 2018; The Water Boiling Test and 4, 2014; Bilsback et al., 2018). For each test, the MOD2 stove was initially at ambient temperature ("cold"), and a new fire was lit in a cold fuel bed (kindling). The stove was fueled with Douglas Fir wood cut into uniform 25 × 25 x 152-mm (1 × 1 x 6-inch) pieces and allowed to dry to 7–9% moisture content on a wet basis. Wood pieces were fed into the combustion chamber lengthwise, with one end slightly protruding from the open feed. The fuel feed rate was controlled to maintain a constant firepower setting of ~5 kW (monitored using real-time CO_2 concentration measurements from the exhaust duct) while bringing 5 L of cold water to a temperature of 99 °C, the nominal local boiling point. Secondary air came from a compressed air cylinder. The standard volumetric flow rate (SLPM) of secondary air was measured using a rotameter, and adjusted using a valve. The secondary air flow was initiated ~2 min after fuel ignition, once the kindling was observed to be fully lit, and was held constant throughout the remainder of the test. The secondary air temperature was monitored every second (1 Hz) using a thermocouple installed inside the stove manifold (Fig. 1(c)). Manifold pressures were measured with a digital manometer through a dedicated tap.

2.3. Parametric testing procedure

Four MOD2 stove design parameters were systematically varied over a total of 111 tests: (1) secondary air injection pattern (2) secondary air injection flow rate (3) primary air intake, and (4) pot height. The first 52 tests were conducted to constrain the parametric space. Two promising air injection patterns were identified during these preliminary tests, shown in Fig. A4 (a total of 7 patterns were tested). Pattern 1 consisted of two concentric rows, each with three orifices evenly spaced around the circumference of the conical chimney. The bottom row of orifices was located just above the firebox, while the top was directly below the throat. Pattern 2 was identical, except that the bottom row had six evenly spaced orifices, rather than three. All air injection orifices had a diameter of 1.59 mm (0.0625 inch). The primary air intake (the size of the inlet area under the grate) and pot height were also set during the preliminary tests, according to the experimental procedures and results provided in the SI.

For the remaining 59 parametric tests, the primary air intake was set to the fully open position and the pot height was held at 25 mm (except for the first 13 tests, when the pot was set 2–5 mm lower). Using these settings, both air injection patterns were tested at six secondary air flow rate settings ranging from 14 to 50 SLPM (0.5–1.75 SCFM), for a total of 12 parametric configurations. Four to eight replicate tests were conducted at each configuration (except for Pattern 2 at 50 SLPM, with only 2 tests). When calculating configuration-average performance and emission metrics using this number of replicate tests, corresponding two-sided 90% confidence intervals were most often <20% (±10%) of the configuration-average values. This level of statistical confidence was deemed sufficient to enable meaningful comparisons. During testing, we discovered that the stove's air manifold leaked at the juncture between the removable conical chimney and the stove body (Fig. A2). However, the leakage was consistent and replicable, and so the secondary flow actually injected into the firebox could be accurately calculated (see the procedure outlined in the SI). The calculations show that 27%–39% of the total secondary flow was injected through the holes in the conical chimney, while the remainder leaked through the faulty manifold juncture, away from the firebox and combustion process. All results are presented in terms of the standard flow rate (SLPM) of air injected into the firebox, ranging from 5.5 to 14 SLPM, rather than the total flow into the manifold.

2.4. Data analysis and performance metrics

All stove performance and emission metric calculations are presented in section S-1.4 of the SI. Emission factors are normalized by the average thermal power delivered to the pot, known as cooking power (kWd). All data are presented with 90% confidence intervals calculated using Student's t-distribution (Wang et al., 2014; Taylor, 1997). The MOD2 stove's performance and emissions are compared to those of the MOD stove (version 1) and a TSF, both tested using the same experimental procedure, fuel, cooking pot, and firepower setting (~5 kW) (Caubel et al., 2018; Rapp et al., 2016). All size-resolved particle emission measurements from the TSI 3321 APS are converted from aerodynamic to electrical mobility diameter, and combined with measurements from the TSI 3091 FMPS according to the methods outlined in Appendix A.

For both air injection patterns, the manifold pressure was measured at each secondary flow rate setting while the stove was cold, as described in Appendix A. Using real-time manifold temperature measurements and Equation (1) below, stove manifold pressures during each test were extrapolated from the corresponding pressure measurement recorded while the stove was cold.

$$\Delta P(t) = \Delta P_{STP}\left(\frac{\rho_{STP}}{\rho(t)}\right) = \frac{\Delta P_{STP}\rho_{STP}(T_{man}(t)+273)R_{air}}{P_{man}} \quad (1)$$

ΔP(t) (Pa) is the manifold gauge pressure at sample time 't', ΔP_{STP} (Pa) is the manifold gauge pressure measured at ambient conditions (show in Fig. A6), ρ_{STP} is the density of air at standard conditions (1.225 kg/m^3), $T_{man}(t)$ (°C) is the air temperature in the manifold at sample time 't', R_{air} is the ideal gas constant for air (287 J/kg K), and P_{man} is the absolute pressure in the manifold (roughly equal to the local ambient pressure, 97150 Pa). Average manifold pressures represent the mean of all 1-s values calculated over the length of the cold start test.

3. Results and discussion

3.1. Stove performance and emissions: air injection pattern and flow rate

For both air injection patterns, Fig. 2 shows that the MOD2 stove's thermal and emissions performance improve significantly as the secondary flow rate increases from 5.3 to 8.5 SLPM. Since firepower was held constant throughout testing, the average stoichiometric flow of air into the combustion reaction is ~70 SLPM for all design configurations (Fig. B4), and the total flow of air through the stove may be 2–5 times higher than this stoichiometric value, as the wood combustion draws excess primary air (Nussbaumer, 2003; Bäfver et al., 2011; Houshfar

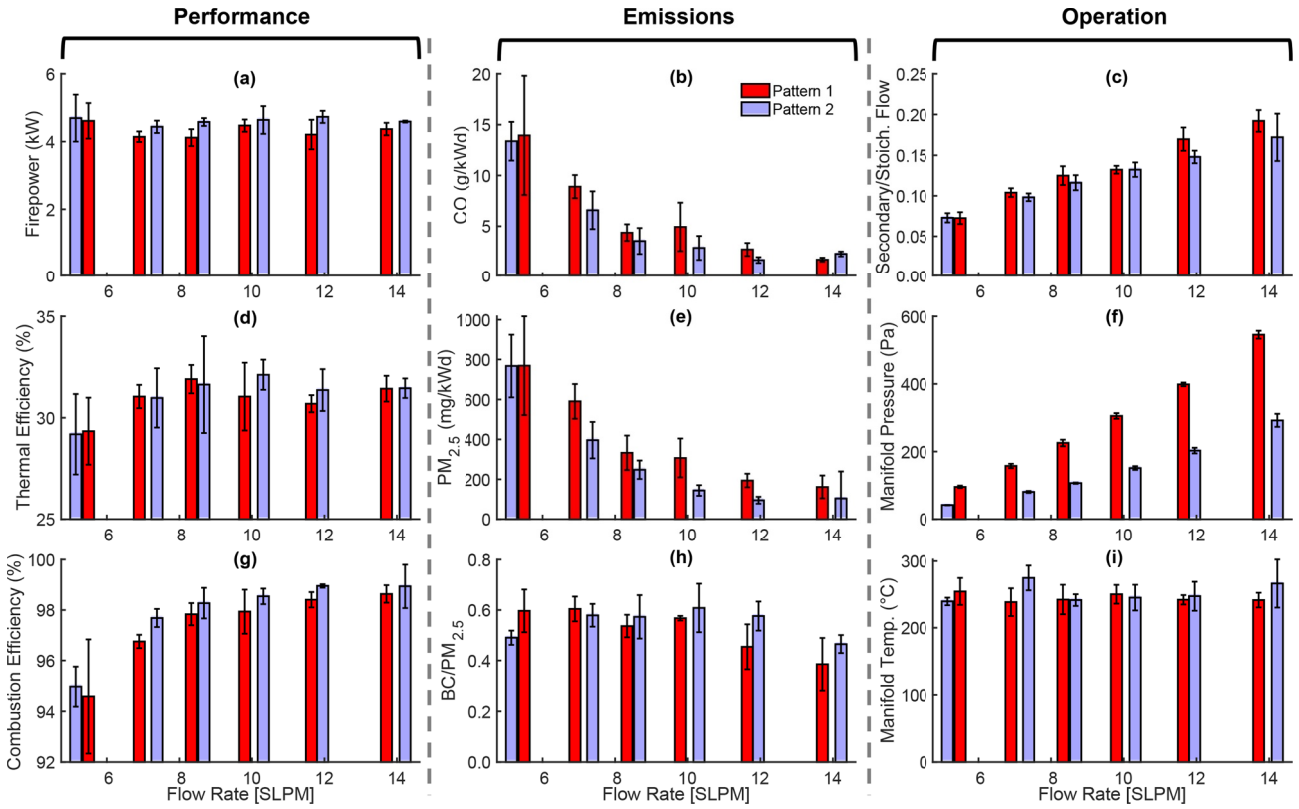

Fig. 2. MOD2 stove performance, emissions, and operational metrics during high-power cold start testing, presented as function of secondary air injection pattern and flow rate: (a) Firepower (kW); (b) Carbon Monoxide (CO) emissions (g/kWd); (c) Ratio of the secondary to stoichiometric flow rate of air; (d) Thermal efficiency (%); (e) Particulate matter ($PM_{2.5}$) emissions (mg/kWd); (f) Average manifold pressure (Pa); (g) Combustion efficiency (%); (h) Black Carbon (BC) to total $PM_{2.5}$ ratio; (i) Average manifold temperature (°C). Bars represent the mean of replicate test data collected for each stove configuration, while error bars represent the corresponding 90% confidence interval.

et al., 2011). Over this range of secondary flow rates, which account for 7.5–12% of the average stoichiometric air flow, CO, $PM_{2.5}$, and BC emissions drop by 55%–75%, while combustion efficiency rises from 95% to 98%. These improvements demonstrate that unprocessed wood combustion is highly sensitive to small changes in secondary flow (relative to the total combustion flow), as higher air jet velocities provide more turbulent mixing and oxygen in the combustion zone (Okasha, 2007). The improvement of combustion conditions also translates to gains in thermal efficiency, which increases from 29% to 32% over this range.

For secondary flow rates above 8.5 SLPM, thermal efficiency remains constant around 31%. At these settings, the secondary flow represents 12–18% of the average stoichiometric flow of air and is much colder than the exhaust gases. The average manifold temperature is roughly 250 °C for all configurations, while exhaust temperatures from biomass combustion typically exceed 850 °C (Lyngfelt and Leckner, 1999; Nussbaumer, 2003). Although the secondary air represents a small fraction of the total air flow into the stove, it may be sufficient at these settings (>8.5 SLPM) to cool the exhaust gases appreciably, thereby limiting the rate of heat transfer to the pot. Other biomass cookstove studies show that exhaust temperatures drop with increased secondary flow (Lyngfelt and Leckner, 1999; Pettersson et al., 2010; Kirch et al., 2018).

Some of the fire's thermal power output is also used to heat the secondary air in the manifold. Since average secondary air temperatures remain approximately constant for all configurations, more heat from the fire is necessarily transferred to the manifold as secondary flow increases. However, Fig. B4 shows that less than 0.1 kW is lost to heating the secondary air at all flow rates, which is small compared to the average thermal power delivered to the pot (~1.4 kW). Therefore, secondary flow does not need to be constrained to maintain high air injection temperatures or prevent the diversion of output heat from the pot to the secondary air manifold, though some restraint is required to prevent excessive cooling of the exhaust gases.

Although thermal performance gains diminish with secondary flow rates above 8.5 SLPM, CO, $PM_{2.5}$, and BC emissions generally decrease steadily throughout the parametric range (Fig. 2 and Fig. B4), thereby suggesting that combustion temperatures remain sufficiently elevated to oxidize harmful pollutants, and higher air injection velocities continue to enhance mixing of the air and gas-phase fuel. Correspondingly, combustion efficiency increases from 98 to 99% as secondary flow rate increases above 8.5 SLPM, representing a further ~50% reduction in the fraction of carbon emitted as a product of incomplete combustion (CO). However, average emissions of CO and $PM_{2.5}$ from Pattern 2 increase slightly at a flow rate of 14 SLPM. While only two tests were conducted in this configuration, the results suggest that secondary flow rates above 12 SLPM through Pattern 2 may quench the flames, and reduce combustion zone temperatures below the 850 °C required to oxidize CO and many of the volatile organic species that form PM (Lyngfelt and Leckner, 1999; Okasha, 2007; Pettersson et al., 2010). However, BC emissions continue to decrease in this stove configuration, as the oxidation temperature of BC is much lower (~350 °C) than that of CO and other pollutants (Elmquist et al., 2006; Jiang et al., 2011), and higher air injection velocities inhibit the formation of fuel-rich flame zones where BC is formed (Bond et al., 2013; Obaidullah et al., 2012).

Emission reductions are not solely dependent on higher secondary air injection velocities to enhance the combustion process. At each flow rate setting, the average injection velocity is roughly 1.5 times greater through Pattern 1 than Pattern 2 (Fig. B4), and yet Fig. 2 shows that Pattern 2 generally outperforms Pattern 1. This trend suggests that the addition of air jets near the fuel bed promotes more effective turbulent mixing in the combustion zone, despite the drop in injection velocity. In

this way, wood combustion is also highly sensitive to the number of secondary air injection orifices and their location relative to the fuel bed, and this sensitivity can be exploited to enhance stove performance. For example, Fig. 2 shows that the manifold pressure at each flow rate setting is 1.9–2.3 times lower for Pattern 2 than for Pattern 1 (theoretically, the manifold pressure should be 2.25 times lower, as the air injection area 1.5 times greater). As a result, greater performance improvements are possible using lower secondary flow rates and pressures that can be more easily provided by the miniature fans and blowers typically found in improved cookstoves.

Fig. 2 shows that a secondary flow rate of 12 SLPM through Pattern 2 minimizes the MOD2 stove's CO and $PM_{2.5}$ emissions, while maximizing combustion efficiency. Although thermal efficiency and BC emissions improve slightly ($\leq$10% relative change) at other flow rate settings, this configuration likely provides an optimal balance between reducing harmful emissions and improving thermal performance. In this configuration, the MOD2 stove emits 90% less CO, $PM_{2.5}$, and BC than a TSF (on average), and thermal efficiency increases from 23 $\pm$ 1% to 31 $\pm$ 1% (Table S1).

While the MOD2 stove can be optimized to reduce biomass smoke emissions by roughly one order of magnitude (relative to a TSF), the ratio of BC to total $PM_{2.5}$ emissions ranges from 0.4 to 0.6 throughout the parametric range, which is higher than that typically reported for biomass cookstoves, both traditional and improved (Vicente and Alves, 2018; Soneja et al., 2015; Garland et al., 2017; Tissari et al., 2008). Initially, we suspected that these unusually elevated BC emission measurements might be the result of instrumentation error, although the Aethalometer was calibrated by the manufacturer prior to both experimental testing phases. Using calibration factors from the manufacturer and fundamental equations, we correctly replicated the instrument's BC concentration outputs from the underlying optical absorption and sample flow rate measurements. During this validation process, we did not uncover any indication that the instrument was operating incorrectly. Taken at face value, the high proportion of BC detected in the MOD2 stove emissions indicates that incomplete oxidation conditions persist (Nuutinen et al., 2014; Vicente and Alves, 2018; Torvela et al., 2014). However, BC is readily oxidized, and can be mitigated through improvements in the combustion process (Obernberger et al., 2007). Therefore, it is important to identify the physical mechanisms responsible for these BC emissions such that they can be actively targeted in future designs.

The BioLite™ HomeStove™ is a wood-burning cookstove similar to the MOD2 stove that emits ~80% less $PM_{2.5}$ than the TSF presented here, and also has elevated BC/$PM_{2.5}$ ratios (>0.7) (Jetter and Ebersviller, 2015). These results suggest that rocket-style cookstoves with secondary air injection may oxidize most PM-forming species, but BC generation somehow persists. A likely explanation for these persistent BC emissions is that the water-filled cooking pot is quenching flames protruding from the chimney throat (Nielsen et al., 2017). When the MOD2 stove was operated without a pot skirt during preliminary tests, Figs. B1 and B4 show that $PM_{2.5}$ emissions were comparable, but BC emissions were 2–3 times lower. Therefore, the BC/$PM_{2.5}$ ratio was significantly reduced (<0.25), though thermal efficiency also suffered without the pot skirt (<29%). The pot skirt restricts the exhaust flow to enhance heat transfer, but the resultantly higher exhaust velocities entrain more flames through the chimney throat, where fuel-rich zones quench against the pot and emit BC. These results motivate further investigations that focus on preventing flame contact with the pot to reduce BC emissions while maintaining high thermal efficiency.

Compared to the MOD stove (version 1), the MOD2 stove achieves similar emission reductions at half the secondary air injection flow rate. Furthermore, when the secondary flow rate was set 25% higher than the optimal setting, $PM_{2.5}$ and CO emissions from the MOD stove more than doubled (Caubel et al., 2018). MOD2 stove emissions, on the other hand, increase only slightly (<40%) when the flow rate rises by ~17%, from 12 SLPM to 14 SLPM. Together, these trends illustrate that the MOD2 stove's smaller firebox and chimney dimensions allow the secondary air jets to be more effective at lower flow rates, penetrating further into the firebox to enable significant emission reductions while preventing excessive cooling or quenching of the combustion. Additionally, the lower secondary flow rates likely contribute to the MOD2 stove's higher thermal efficiency, as cooling of the exhaust flow diminishes.

Together, the experimental results demonstrate that the secondary air injection pattern and flow rate must be optimized to maximize the effective jet velocity but prevent flame quenching. Design compromises are also sometimes required to enhance both the stove's thermal and emissions performance. In this case, adding a pot skirt to the MOD2 stove enhanced thermal efficiency but also increased the BC/$PM_{2.5}$ ratio. Since the MOD2 stove still achieves significant (90 $\pm$ 10%) BC mass emission reductions relative to a TSF, the elevated BC/$PM_{2.5}$ ratio may be justified by the increase in thermal efficiency afforded. Having identified the optimal MOD2 stove design configuration and established the underlying physical mechanisms responsible for the performance improvements, it is important to determine whether these experimental results can be translated into a practical cookstove design that households can afford and adopt.

3.2. Secondary air injection design requirements: flow, pressure and power

The MOD2 stove receives pressurized air from a cylinder, such that the secondary flow can be adjusted accurately and consistently over the course of many experimental trials, but this approach is clearly not practical or economical for typical household applications. Instead, many commercial biomass cookstoves rely on a small axial fan or centrifugal blower to drive the secondary flow, often drawing electrical power from a thermoelectric generator (TEG) (Jetter and Ebersviller, 2015; Sutar et al., 2015). TEGs convert heat from the biomass combustion directly to electricity, thereby providing an independent, reliable, and convenient source of power at little cost (often < $10/W of power generated) (Champier et al., 2010, 2011; Gao et al., 2016; Nuwayhid et al., 2005). TEG modules mounted to biomass cookstoves have been shown to generate as much as 10 W of electrical power, although an output of 1–5 W is more typical (Champier et al., 2011; Gao et al., 2016; Nuwayhid et al., 2005; Mal et al., 2015). There are also some biomass cookstoves powered by solar panels or simple wall chargers, but these alternatives are often less desirable, as they depend on operational factors external to the cookstove (such as sufficient insolation).

Fig. 2 shows that MOD2 performance is optimal when injecting a secondary flow rate of 12 SLPM through Pattern 2. In this configuration, an average manifold pressure of ~200 Pa is required. As the stove heats up during normal use, higher manifold pressure is required to maintain a constant mass flow of secondary air through the injection pattern. Air is injected into the MOD stove at room temperature (~25–30 °C) throughout, but reaches manifold temperatures of 300–400 °C during the cold start test (Fig. 5). The density of air at these elevated temperatures is around half that of the air initially flowing into the manifold, and so the volumetric flow rate passing through the injection pattern effectively doubles, as does the manifold pressure required. Consequently, when sizing a fan or blower to drive secondary air injection in a biomass cookstove, it is important to consider the manifold pressure required at typical operating conditions, rather than when the stove is cold (at ambient temperature). In this study, we defined the operating temperature as the average secondary air temperature in the manifold during the cold start, and therefore we also present the average manifold pressure.

Fig. 3 provides the maximum (static) pressure, maximum (free) flow rate, and rated electrical power consumption of 1135 miniature fans and blowers stocked by Digi-Key Electronics®, a major electronic parts supplier (Digi-Key Electronics, 2018). This dataset is provided in Appendix B5. All available models costing < $10 (when ordering 1000

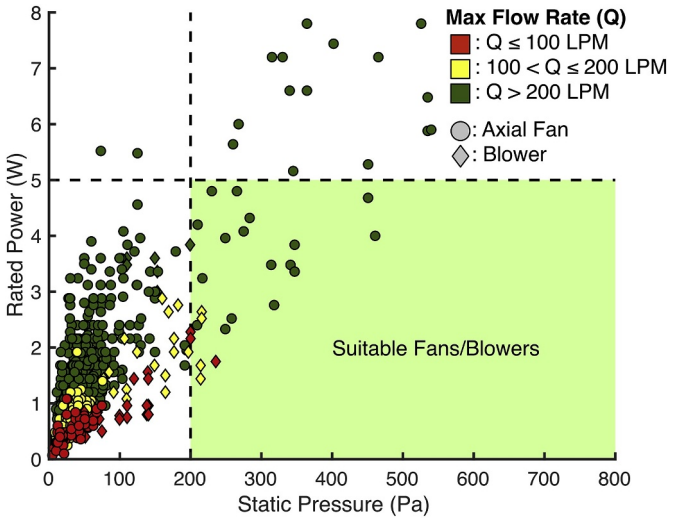

Fig. 3. Static pressure, free flow rate, and rated electrical power consumption of 1135 miniature axial fans and centrifugal blowers that are stocked by Digi-Key Electronics ® and cost < $10 per unit (when ordering 1000 units) (Digi-Key Electronics, 2018). Fans and blowers that meet the MOD2 stove's operational requirements (in the optimal design configuration) are indicated. Marker colors represent the devices' ability to operate near static flow conditions while providing the stove's required flow rate (12 SLPM).

units) are presented, as the minimization of manufacturing costs is crucial to the development of affordable cookstoves. To reflect the MOD2 stove's operational requirements, reference lines are provided at a static pressure of 200 Pa and rated electrical power of 5 W (the maximum power typically output by a stove-mounted TEG module). The devices must operate near static conditions, or at a flow rate below ~10% of the maximum value specified by the manufacturer (measured with no flow resistance), to generate the maximum pressures presented in Fig. 3. The MOD2 stove requires 12 SLPM in the optimal configuration, so the free flow rate should be at least ~100 LPM for the fan or blower to operate near static conditions. This target is based on a rough approximation of actual performance, so fans and blowers with a free flow rating ranging from 100 to 200 LPM (at standard conditions) are represented using yellow markers (Fig. 3) to indicate that some may not satisfy the 12 SLPM requirement under operational conditions. Green markers represent devices that are nearly certain to meet or exceed the stove's secondary flow rate requirement, while red markers indicate devices unlikely to meet the requirements. Since secondary air is drawn into the stove from the environment near standard conditions, the rated volumetric flow rate (LPM) is analogous to the stove's mass flow rate (SLPM) requirements, identified experimentally. It should also be noted that the rated power consumption is often measured at free flow conditions, and though this may not be exactly representative of power consumption at the requisite operating conditions (which will likely be larger as flow resistance is applied), it provides a valid estimate.

Only 23 (~2%) of the 1135 fans and blowers presented in Fig. 3 meet the MOD2 stove's static pressure (>200 Pa), free flow (>100 SLPM), and electrical power (<5 W) requirements. Miniature fans and blowers are typically designed for cooling electronics, and therefore provide high air flow rates at low pressures – over 70% of the devices shown in Fig. 3 generate maximum flow rates >100 LPM using <5 W of power, but at static pressures <100 Pa. However, the MOD2 stove requires relatively low flow rates of air, driven through small orifices that generate high velocity air jets in the combustion chamber, but require high input pressures.

The small proportion of suitable fans and blowers illustrates the importance of carefully characterizing the cookstove's operational requirements. Using only knowledge of the air injection flow rate, as is usually provided in existing experimental studies, it is straightforward to select a fan or blower that meets the flow requirement, but provides insufficient positive pressure. Similarly, without manifold temperature measurements, it would be difficult to discern that the cookstove's volumetric flow rate and manifold pressure requirements double during normal operation. This analysis suggests that poorly performing cookstoves with secondary air injection may suffer from the implementation of inadequate fans and blowers, as operational guidelines are lacking.

Of the 23 viable devices identified, Fig. 3 shows that suitable blowers generally require less power than axial fans, as they are better suited to high pressure, low flow applications. Overall, Fig. 3 illustrates that low-cost fans and blowers are currently available to achieve effective and practical secondary air injection in wood-burning cookstoves, but they must be carefully chosen and evaluated, as the vast majority are not

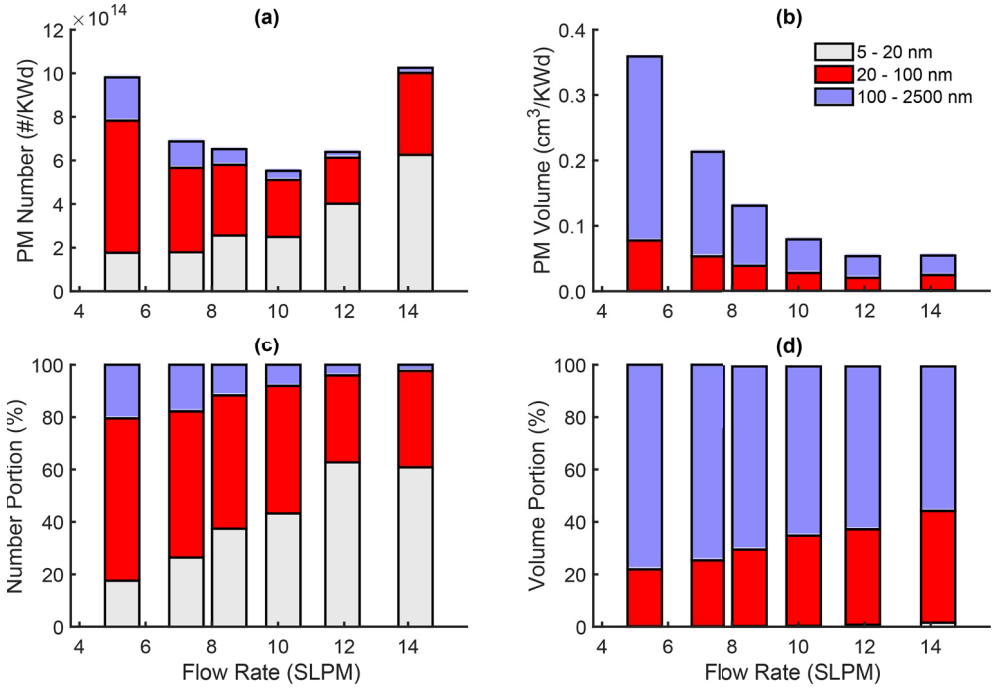

Fig. 4. (a) Total $PM_{2.5}$ number and (b) volume emissions from the MOD2 stove over the cold start (normalized by cooking power), as a function of particle diameter and secondary flow rate through air injection Pattern 2. (c) Portion of the total number, and (d) volume of particles emitted in each particle diameter range: 5–20 nm, 20–100 nm, and 100–2500 nm. Each bar represents the mean of replicate test data collected for each stove configuration. Confidence intervals are omitted here for clarity, and instead provided in Fig. B5.

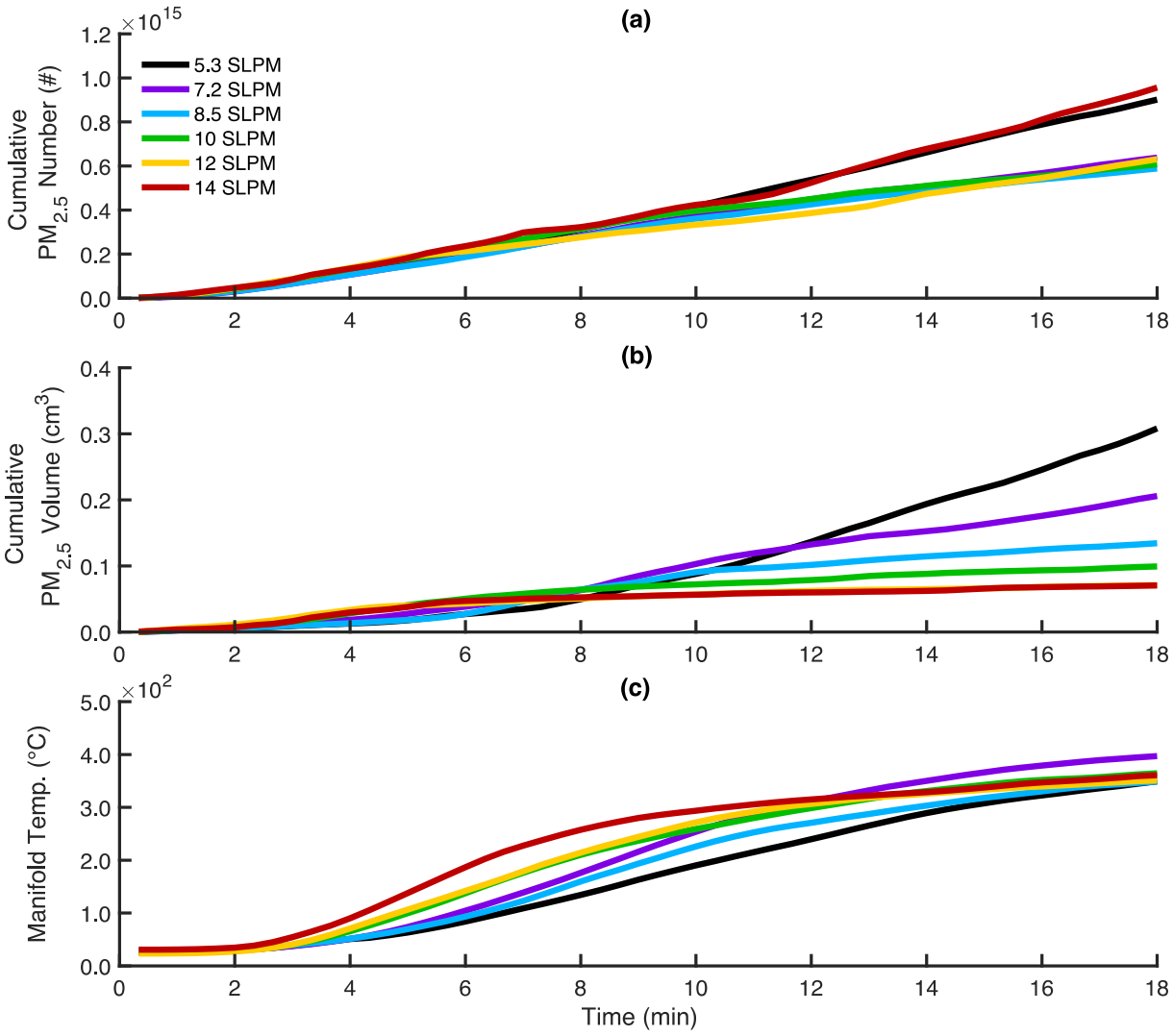

Fig. 5. (a) Accumulation of $PM_{2.5}$ number and (b) volume emissions from the MOD2 stove over the first 18 min of the cold start test. (c) Temperature of secondary air in the MOD2 stove manifold over the same period. Each line represents the mean of replicate test measurements collected at each of the six secondary flow settings (using air injection Pattern 2). Confidence intervals are omitted here for clarity, and instead provided in Figs. B7 and B8 for all secondary flow rate settings. All data presented is block-averaged on a 20-sec time base.

intended to meet the flow, pressure, and electrical power consumption conditions required.

3.3. Room for improvement: start up and ultrafine particle emissions

Health guidelines from the WHO, United States Environmental Protection Agency (US EPA), and other organizations generally recommend maximum $PM_{2.5}$ pollution levels in terms of mass concentration (e.g., $\mu g/m^3$). By this measure, the MOD2 stove should alleviate health impacts from biomass combustion, as it reduces $PM_{2.5}$ mass emissions by an order of magnitude relative to a traditional TSF. However, Fig. 4 shows that the vast majority (>80%) of $PM_{2.5}$ emissions from the MOD2 stove consist of ultrafine particles (UFP) with a diameter < 100 nm, which may be particularly harmful to human respiratory health, as their small size enables deeper penetration into the lungs (Valavanidis et al., 2008; Martins et al., 2010; Chen et al., 2016b; Clifford et al., 2018). Consequently, it is important not only to reduce the mass of PM generated, but also the number of UFPs emitted and potentially inhaled.

Secondary air injection does not significantly reduce the total number of particles generated by biomass combustion, but instead shifts the PM size distribution towards smaller, less massive particles (Caubel et al., 2018; Rapp et al., 2016; Just et al., 2013; Shen et al., 2017). As the secondary flow rate increases from 7.2 to 12 SLPM, Fig. 4 shows that the total number of particles emitted from 5 to 2500 nm remains relatively steady, ranging from 5.5×10^{14} to 6.9×10^{14} particles/kWd. Total $PM_{2.5}$ vol, on the other hand, decreases over the range of secondary flow rates presented, as particle size diminishes. Given that $PM_{2.5}$ density remains nearly constant (Fig. B4), the particle volume measurements are directly proportional to particle mass, and therefore closely mirror the $PM_{2.5}$ mass emission measurements shown in Fig. 2.

Fig. 4 shows that secondary air injection inhibits particle growth, but does not significantly reduce particle formation. Particles form either through nucleation, as volatile organic and inorganic compounds emitted during wood pyrolysis cool in the exhaust, or through soot (BC) generation in the flame (Lamberg et al., 2011; Obaidullah et al., 2012; Obernberger et al., 2007; Kelz et al., 2010). Typically, these primary particles grow through agglomeration and condensation of volatile compounds. Fig. 2 shows that CO and $PM_{2.5}$ mass reductions closely mirror one another as secondary flow rate increases, likely because CO and many-PM forming volatile organic compounds (e.g. PAH) oxidize under similar conditions (Tissari et al., 2008; Torvela et al., 2014; Johansson et al., 2004). The portion of PM in the nucleation mode (5–20 nm) increases from 20 to 60% as secondary air flow through Pattern 2 increases, likely because particles no longer grow by condensation as

volatile organic gas emissions diminish. While number emissions of these small particles increase markedly, they account for less than 2% of the total PM volume, and therefore have little effect on the total mass emitted. Fig. B9 provides the size distribution of particle number emissions, and shows a distinct peak at a particle diameter of ~12 nm that increases with secondary flow rate.

In the absence of volatile organic gases in the exhaust, inorganic and BC particles generally grow to sizes <100 nm through agglomeration (Bond et al., 2013; Torvela et al., 2014; Nielsen et al., 2017; Wiinikka and Gebart, 2005). Fig. 4 shows that the fraction of total particle number emissions in the UFP range (5–100 nm) grows from 80 to 97% as secondary flow increases, and accounts for 20–40% of the PM volume generated. As the size distribution shifts towards smaller particles, the fraction of particles in the accumulation mode (100–2500 nm) correspondingly decreases from 20 to 3% over the parametric range presented, but still accounts for most (60–80%) of the emitted volume. Particles in the accumulation mode form as some growth pathways persist, such the condensation of gases in cool regions of the exhaust flow or agglomeration of particles under turbulent mixing conditions. Throughout the parametric range, nearly all (» 99.9%) particles emitted are smaller than 1000 nm (6). Larger particles (>1000 nm) account for 0.2–0.7% of the total particle volume, and likely consist of fly ash generated in the fuel bed and entrained in the exhaust flow (Obaidullah et al., 2012).

Total particle number emissions are lowest for a secondary flow rate of 10 SLPM (Fig. 4), suggesting that this configuration may provide the optimal balance of turbulent mixing and high combustion temperatures to inhibit particle formation. However, total $PM_{2.5}$ vol generation continues to decrease at higher flow rates, as particle size diminishes. Furthermore, $PM_{2.5}$ number emissions increases sharply from 12 to 14 SLPM, again indicating that excessive secondary flow in this configuration quenches the combustion zone (Nuutinen et al., 2014), thereby promoting more PM nucleation. However, total $PM_{2.5}$ vol changes little, as PM emissions in the accumulation mode remain relatively constant. Together, these trends demonstrate that $PM_{2.5}$ mass emission reductions can be achieved while simultaneously generating more UFPs.

When the secondary air flow rate is sufficient, the particle size distribution increasingly shifts towards smaller, less massive particles as the stove, fuel, and exhaust gases warm up during the cold start test (Hosseini et al., 2010). The injection of hotter secondary air at higher velocities also likely contributes to the shift towards smaller particle emissions, as injection velocity increases proportionally with manifold temperature (Equation A5). When the secondary flow rate setting through Pattern 2 increases, Fig. 5 shows that particle volume generation is increasingly attenuated over the first 18 min of the cold start test, although the number of emitted particles accumulates steadily for all configurations. The $PM_{2.5}$ number and volume accumulation rates reflect the secondary flow dependence illustrated in Fig. 4. Manifold temperatures rise more rapidly at higher flow rate settings (Fig. 5(c)), thereby hastening the inhibition of particle growth. For flow rates ≥10 SLPM, the count median diameter (CMD) of particle emissions decreases from around 60 nm–20 nm over the first 18 min of the cold start (Fig. B10), and so most of the particle volume is emitted during start up. At the optimal secondary flow rate setting of 12 SLPM, half of total volume emissions are emitted within the first ~7 min following ignition, representing only ~30% of the total test length (in this configuration, the average time to boil is 24 ± 2 min). Consequently, if further PM mass reductions are sought, methods should be developed to enhance combustion conditions during start up.

Although volume emissions are attenuated over time, the number of particles continues to accumulate steadily for all configurations, and the CMD is less <80 nm throughout (Fig. B10), well within the ultrafine range that is of particular concern for human health. As a result, it is important that future research efforts investigate methods for inhibiting particle formation entirely, rather than simply limiting particle growth. For example, methods of restricting the fuel bed temperature could be devised to limit the volatilization of inorganic compounds that nucleate into incombustible particles (Lamberg et al., 2011).

4. Conclusion

While further improvements are needed to reduce UFP emissions, the MOD2 stove generally illustrates that secondary air injection is a practical and effective method for reducing mass emissions of $PM_{2.5}$, CO, and BC from wood combustion. Crucially, we show that emission reductions are achievable using inexpensive hardware that is currently on the market, and can be driven independently using a TEG or other low-cost power source. Stove performance is highly sensitive to secondary air injection design parameters, and so it is important that new designs be validated and optimized experimentally. The experimental results presented here illustrate important design principles that will help to inform the development of clean, efficient, and practical cookstoves that better mitigate harmful air pollution exposure in the billions of households that depend on solid biomass for their daily cooking needs.

Declaration of competing interest

None.

Acknowledgment

This work was performed at the Lawrence Berkeley National Laboratory, operated by the University of California, under DOE Contract DE-AC02-05CH11231. We gratefully acknowledge support for this work from DOE's Biomass Energy Technologies Office. Author Julien J. Caubel is grateful for support from the National Science Foundation's Graduate Research Fellowship Program Contract No. 1106400.

The authors would like to recognize the central contribution of Allen Boltz, Marion Laglaive, Guillaume Charbonnel, Varun Khurana, Maelle Seigle and Anouar Mabrouk, who spent countless hours in the laboratory testing the cookstove and collecting the experimental data upon which this research is founded. We would also like to acknowledge the engineering staff at UC Berkeley and Lawrence Berkeley National Laboratory who fabricated the cookstove hardware: Alex Jordan, Jacob Gallego, Jeffrey Olson, Tim Williams, and Rick Kraft. Finally, we thank Dr. Daniel Wilson for his guidance in post-processing the particle emissions data and Gary Hubbard for developing the software tools to simplify data collection from all of our instruments.

Appendices A and B. Supplementary Data

Supplementary data to this article can be found online at https://doi.org/10.1016/j.deveng.2020.100049.

References

Bäfver, L.S., Leckner, B., Tullin, C., Berntsen, M., 2011. Particle emissions from pellets stoves and modern and old-type wood stoves. Biomass Bioenergy 35 (8), 3648–3655.

Bilsback, K.R., Eilenberg, S.R., Good, N., Heck, L., Johnson, M., Kodros, J.K., Lipsky, E. M., L'Orange, C., Pierce, J.R., Robinson, A.L., Subramanian, R., Tryner, J., Wilson, A., Volckens, J., 2018. The firepower sweep test: a novel approach to cookstove laboratory testing. Indoor Air 28 (6), 936–949.

Bond, T.C., Doherty, S.J., Fahey, D.W., 2013. Bounding the role of black carbon in the climate system: a scientific assessment. J. Geophys. Res. Atmos. 118 (11), 5380–5552.

Bonjour, S., Adair-Rohani, H., Wolf, J., Bruce, N.G., Mehta, S., Prüss-Ustün, A., Lahiff, M., Rehfuess, E.A., Mishra, V., Smith, K.R., 2013. Solid fuel use for household cooking: country and regional estimates for 1980–2010. Environ. Health Perspect. 121 (7), 784–790.

Bruce, N.G., Perez-Padilla, R., Albalak, R., 2000. Indoor air pollution in developing countries: a major environmental and public health challenge. Bull. World Health Organ. 78 (9), 1078–1092.

Caubel, J.J., Rapp, V.H., Chen, S.S., Gadgil, A.J., 2018. Optimization of secondary air injection in a wood-burning cookstove: an experimental study. Environ. Sci. Technol. 52 (7), 4449–4456.

Champier, D., Bedecarrats, J.P., Rivaletto, M., Strub, F., 2010. Thermoelectric power generation from biomass cook stoves. Energy 35 (2), 935–942.

Champier, D., Bédécarrats, J.P., Kousksou, T., Rivaletto, M., Strub, F., Pignolet, P., 2011. Study of a TE (thermoelectric) generator incorporated in a multifunction wood stove. Energy 36 (3), 1518–1526.
Chen, C., Zeger, S., Breysse, P., Katz, J., Checkley, W., Curriero, F.C., Tielsch, J.M., 2016a. Estimating indoor PM2.5 and CO concentrations in households in southern Nepal: the Nepal cookstove intervention trials. PloS One 11 (7) e0157984–17.
Chen, R., Hu, Bin, Liu, Y., Xu, J., Yang, G., Xu, D., Chen, C., 2016b. Beyond PM2.5: the role of ultrafine particles on adverse health effects of air pollution. BBA - General Subjects 1860 (12), 2844–2855.
Clifford, S., Mazaheri, M., Salimi, F., Ezz, W.N., Yeganeh, B., Low-Choy, S., Walker, K., Mengersen, K., Marks, G.B., Morawska, L., 2018. Effects of exposure to ambient ultrafine particles on respiratory health and systemic inflammation in children. Environ. Int. 114, 167–180.
Cushman-Roisin, B., 2014. Turbulent jets. In: Environmental Fluid Mechanics; New York, pp. 1–9.
Delapena, S., Garland, C., Jagoe, K., Okada, E., Ouk, S., Pennise, D., Pillarisetti, A., Steele, J., 2015. Quantifying the Health Impacts of ACE-1 Biomass and Biogas Stoves in Cambodia. Berkeley Air Monitoring Group, pp. 1–52.
Digi-Key Electronics. Fans and thermal management: DC brushless fans (BLDC). http://www.digikey.com/products/en/fans-thermal-management/dc-brushless-fans-bldc/217?. (Accessed 12 September 2018).
Edwards, R., Karnani, S., Fisher, E.M., Johnson, M., Naeher, L., Smith, K.R., Morawska, L., 2014. WHO Indoor Air Quality Guidelines: Household Fuel Combustion. World Health Organization, pp. 1–42.
Elmquist, M., Cornelissen, G., Kukulska, Z., Gustafsson, Ö., 2006. Distinct oxidative stabilities of char versus soot black carbon: implications for quantification and environmental recalcitrance. Global Biogeochem. Cycles 20 (2), 1–11.
Foell, W., Pachauri, S., Spreng, D., Zerriffi, H., 2011. Household cooking fuels and Technologies in developing economies. Energy Pol. 39 (12), 7487–7496.
Gao, H.B., Huang, G.H., Li, H.J., Qu, Z.G., Zhang, Y.J., 2016. Development of stove-powered thermoelectric generators: a review. Appl. Therm. Eng. 96, 297–310.
Garland, C., Delapena, S., Prasad, R., L'Orange, C., Alexander, D., Johnson, M., 2017. Black carbon cookstove emissions: a field assessment of 19 stove/fuel combinations. Atmos. Environ. 169, 140–149.
Hosseini, S., Li, Q., Cocker, D., Weise, D., Miller, A., Shrivastava, M., Miller, J.W., Mahalingam, S., Princevac, M., Jung, H., 2010. Particle size distributions from laboratory-scale biomass fires using Fast response instruments. Atmos. Chem. Phys. 10 (16), 8065–8076.
Houshfar, E., Skreiberg, Ø., Løvås, T., Todorović, D., Sørum, L., 2011. Effect of excess air ratio and temperature on NOx emission from grate combustion of biomass in the staged air combustion scenario. Energy Fuels 25 (10), 4643–4654.
Jetter, J., Ebersviller, S., 2015. Test Report: BioLite HomeStove with Wood Fuel. U.S. Environmental Protection Agency, pp. 1–33.
Jetter, J., Zhao, Y., Smith, K.R., Khan, B., Yelverton, T., DeCarlo, P., Hays, M.D., 2012. Pollutant emissions and Energy efficiency under controlled conditions for household biomass cookstoves and implications for metrics useful in setting international test standards. Environ. Sci. Technol. 46 (19), 10827–10834.
Jiang, M., Wu, Y., Lin, G., Xu, L., Chen, Z., Fu, F., 2011. Pyrolysis and thermal-oxidation characterization of organic carbon and black carbon aerosols. Sci. Total Environ. 409 (20), 4449–4455.
Johansson, L.S., Leckner, B., Gustavsson, L., Cooper, D., Tullin, C., Potter, A., 2004. Emission characteristics of modern and old-type residential boilers fired with wood logs and wood pellets. Atmos. Environ. 38 (25), 4183–4195.
Just, B., Rogak, S., Kandlikar, M., 2013. Characterization of ultrafine particulate matter from traditional and improved biomass cookstoves. Environ. Sci. Technol. 47 (7), 3506–3512.
Kelz, J., Brunner, T., Obernberger, I., Jalava, P., Hirvonen, M.R., 2010. PM emissions from old and modern biomass combustion systems and their health effects. In: Proceedings of the 18th European Biomass Conference, Lyon, France, May 2010. ETA - Florence Renewable Energies, Florence, Italy.
Kirch, T., Birzer, C.H., Medwell, P.R., Holden, L., 2018. The role of primary and secondary air on wood combustion in cookstoves. Int. J. Sustain. Energy 37 (3), 268–277.
Lamberg, H., Sippula, O., Tissari, J., Jokiniemi, J., 2011. Effects of air staging and load on fine-particle and gaseous emissions from a small-scale pellet boiler. Energy Fuels 25 (11), 4952–4960.
Legros, G., Havet, I., Bruce, N.G., Bonjour, S., 2009. The Energy Access Situation in Developing Countries. United Nations Development Programme (UNDP), New York, pp. 1–142.
Lienhard, J.H.V., Lienhard, J.H., 1984. IV. Velocity coefficients for free jets FromSharp-edged orifices. J. Fluid Eng. 106 (13), 13–17.
Lyngfelt, A., Leckner, B., 1999. Combustion of wood-chips in circulating fluidized bed boilers — NO and CO emissions as functions of temperature and air-staging. Fuel 78, 1065–1072.
Mal, R., Prasad, R., Vijay, V.K., Verma, A.R., 2015. The design, development and performance evaluation of thermoelectric generator(TEG) integrated forced draft biomass cookstove. Procedia - Procedia Computer Science 52, 723–729.
Malla, S., Timilsina, G.R., 2014. Household Cooking Fuel Choice and Adoption of Improved Cookstoves in Developing Countries. The World Bank, pp. 1–52.
Martins, L.D., Martins, J.A., Freitas, E.D., Mazzoli, C.R., Gonçalves, F.L.T., Ynoue, R.Y., Hallak, R., Albuquerque, T.T.A., Andrade, M. de F., 2010. Potential health impact of ultrafine particles under clean and polluted urban atmospheric conditions: a model-based study. Air Qual Atmos Health 3 (1), 29–39.
Nielsen, I.E., Eriksson, A.C., Lindgren, R., Martinsson, J., Nyström, R., Nordin, E.Z., Sadiktsis, I., Boman, C., Nøjgaard, J.K., Pagels, J., 2017. Time-resolved analysis of particle emissions from residential biomass combustion - emissions of refractory black carbon, PAHs and organic tracers. Atmos. Environ. 165, 179–190.
Nussbaumer, T., 2003. Combustion and Co-combustion of Biomass: fundamentals, Technologies, and primary measures for emission reduction †. Energy Fuels 17 (6), 1510–1521.
Nuutinen, K., Jokiniemi, J., Sippula, O., Lamberg, H., Sutinen, J., Horttanainen, P., Tissari, J., 2014. Effect of air staging on fine particle, dust and gaseous emissions from masonry heaters. Biomass Bioenergy 67, 167–178.
Nuwayhid, R.Y., Shihadeh, A., Ghaddar, N., 2005. Development and testing of a domestic woodstove thermoelectric generator with natural convection cooling. Energy Convers. Manag. 46 (9–10), 1631–1643.
Obaidullah, M., Bram, S., Verma, V.K., De Ruyck, J., 2012. A review on particle emissions from small scale biomass combustion. Int. J. Renew. Energy Resour. 2 (1), 147–159.
Obernberger, I., Brunner, T., Barnthaler, G., 2007. Fine particulate emissions from modern Austrian small-scale biomass combustion plants. In: 15th European Biomass Conference & Exhibition, Berlin, Germany, May 7-11.
Okasha, F., 2007. Staged combustion of rice straw in a fluidized bed. Exp. Therm. Fluid Sci. 32 (1), 52–59.
Pettersson, E., Lindmark, F., Öhman, M., Nordin, A., Westerholm, R., Boman, C., 2010. Design changes in a fixed-bed pellet combustion device: effects of temperature and residence time on emission performance. Energy Fuels 24 (2), 1333–1340.
Rapp, V.H., Caubel, J.J., Wilson, D.L., Gadgil, A.J., 2016. Reducing ultrafine particle emissions using air injection in wood-burning cookstoves. Environ. Sci. Technol. 50 (15), 8368–8374.
Shen, G., Gaddam, C.K., Ebersviller, S.M., Vander Wal, R.L., Williams, C., Faircloth, J.W., Jetter, J.J., Hays, M.D., 2017. A laboratory comparison of emission factors, number size distributions, and morphology of ultrafine particles from 11 different household cookstove-fuel systems. Environ. Sci. Technol. 51 (11), 6522–6532.
Smith, K.R., Dutta, K., Chengappa, C., Gusain, P.P., Masera, O., Berrueta, V., Edwards, R., Bailis, R., Shields, K.N., 2007. Monitoring and evaluation of improved biomass cookstove programs for indoor air quality and stove performance: conclusions from the household Energy and health project. Energy for Sustainable Development 11 (2), 5–18.
Soneja, S.I., Tielsch, J.M., Curriero, F.C., Zaitchik, B., Khatry, S.K., Yan, B., Chillrud, S.N., Breysse, P.N., 2015. Determining particulate matter and black carbon exfiltration estimates for traditional cookstove use in rural Nepalese village households. Environ. Sci. Technol. 49 (9), 5555–5562.
Stanaway, J.D., Afshin, A., Gakidou, E., Lim, S.S., Abate, D., Abate, K.H., Abbafati, C., Abbasi, N., Abbastabar, H., Abd-Allah, F., Abdela, J., Abdelalim, A., Abdollahpour, I., Abdulkader, R.S., Abebe, M., Abebe, Z., Abera, S.F., Abil, O.Z., Abraha, H.N., Abrham, A.R., Abu-Raddad, L.J., Abu-Rmeileh, N.M., Accrombessi, M. M.K., Acharya, D., Acharya, P., Adamu, A.A., Adane, A.A., Adebayo, O.M., Adedoyin, R.A., Adekanmbi, V., Ademi, Z., Adetokunboh, O.O., Adib, M.G., Admasie, A., Adsuar, J.C., Afanvi, K.A., Afarideh, M., Agarwal, G., Aggarwal, A., Aghayan, S.A., Agrawal, A., Agrawal, S., Ahmadi, A., Ahmadi, M., Ahmadieh, H., Ahmed, M.B., Aichour, A.N., Aichour, I., Aichour, M.T.E., Akbari, M.E., Akinyemiju, T., Akseer, N., Al-Aly, Z., Al-Eyadhy, A., Al-Mekhlafi, H.M., Alahdab, F., Alam, K., Alam, S., Alam, T., Alashi, A., Alavian, S.M., Alene, K.A., Ali, K., Ali, S.M., Alijanzadeh, M., Alizadeh-Navaei, R., Aljunid, S.M., Alkerwi, A., Alla, F.O., Alsharif, U., Altirkawi, K., Alvis-Guzman, N., Amare, A.T., Ammar, W., Anber, N.H., Anderson, J.A., Andrei, C.L., Androudi, S., Animut, M.D., Anjomshoa, M., Ansha, M. G., AntÃ³, J.M., Antonio, C.A.T., Anwari, P., Appiah, L.T., Appiah, S.C.Y., Arabloo, J., Aremu, O., v, J.Ã.R., Artaman, Al, Aryal, K.K., Asayesh, H., Ataro, Z., Ausloos, M., Avokpaho, E.F.G.A., Awasthi, A., Quintanilla, B.P.A., Ayer, R., Ayuk, T. B., Azzopardi, P.S., Babazadeh, A., Badali, H., Badawi, A., Balakrishnan, K., Bali, A. G., Ball, K., Ballew, S.H., Banach, M., Banoub, J.A.M., Barac, A., Barker-Collo, S.L., rnighausen, T.W.B., Barrero, L.H., Basu, S., Baune, B.T., Bazargan-Hejazi, S., Bedi, N., Beghi, E., Behzadifar, M., Behzadifar, M., jot, Y.B., Bekele, B.B., Bekru, E.T., Belay, E., Belay, Y.A., Bell, M.L., Bello, A.K., Bennett, D.A., Bensenor, I.M., Bergeron, G., Berhane, A., Bernabe, E., Bernstein, R.S., Beuran, M., Beyranvand, T., Bhala, N., Bhalla, A., Bhattarai, S., Bhutta, Z.A., Biadgo, B., Bijani, A., Bikbov, B., Bilano, Ver, Bililign, N., Bin Sayeed, M.S., Bisanzio, D., Biswas, T., rge, T.B., Blacker, B.F., Bleyer, A., Borschmann, R., Bou-Orm, I.R., Boufous, S., Bourne, R., Brady, O.J., Brauer, M., Brazinova, A., Breitborde, N.J.K., Brenner, H., Briko, A.N., Britton, G., Brugha, T., Buchbinder, R., Burnett, R.T., Busse, R., Butt, Z.A., Cahill, L. E., Cahuana-Hurtado, L., Campos-Nonato, I.R., rdenas, R.C., Carreras, G., Carrero, J. J., Carvalho, F.L., eda-Orjuela, C.A.C., Rivas, J.C., Castro, F., pez, F.N.C.L., Causey, K., Cercy, K.M., Cerin, E., Chaiah, Y., Chang, H.-Y., Chang, J.-C., Chang, K.-L., Charlson, F.J., Chattopadhyay, A., Chattu, V.K., Chee, M.L., Cheng, C.-Y., Chew, A., Chiang, P.P.-C., Chimed-Ochir, O., Chin, K.L., Chitheer, A., Choi, J.-Y.J., Chowdhury, R., Christensen, H., Christopher, D.J., Chung, S.-C., Cicuttini, F.M., Cirillo, M., Cohen, A.J., Collado-Mateo, D., Cooper, C., Cooper, O.R., Coresh, J., Cornaby, L., Cortesi, P.A., Cortinovis, M., Costa, M., Cousin, E., Criqui, M.H., Cromwell, E.A., Cundiff, D.K., Daba, A.K., Dachew, B.A., Dadi, A.F., Damasceno, A. A.M., Dandona, L., Dandona, R., Darby, S.C., Dargan, P.I., Daryani, A., Gupta Das, R., Neves das, J., Dasa, T.T., Dash, A.P., Davitoiu, D.V., Davletov, K., ngora, la Cruz-GÃ., De, V., La, Hoz, De, F.P., De Leo, D., De Neve, J.-W., Degenhardt, L., Deiparine, S., Dellavalle, R.P., Demoz, G.T., rrez, E.D.-G., Deribe, K., Dervenis, N., Deshpande, A., Jarlais, Des, D.C., Dessie, G.A., Deveber, G.A., Dey, S., Dharmaratne, S.D., Dhimal, M., Dinberu, M.T., Ding, E.L., Diro, H.D., Djalalinia, S., Do, H.P., Dokova, K., Doku, D.T., Doyle, K.E., Driscoll, T.R., Dubey, M., Dubljanin, E., Duken, E.E., Duncan, B.B., Duraes, A.R., Ebert, N., Ebrahimi, H., Ebrahimpour, S., Edvardsson, D., Effiong, A., Eggen, A.E., Bcheraoui El, C., El-Khatib, Z., Elyazar, I.R., Enayati, A., Endries, A.Y., Er, B., Erskine, H.E., Eskandarieh, S., Esteghamati, A., Estep, K., Fakhim, H., Faramarzi, M., Fareed, M., Farid, T.A., Farinha, C.S.E.S., Farioli, A.,

Faro, A., Farvid, M.S., Farzaei, M.H., Fatima, B., Fay, K.A., Fazaeli, A.A., Feigin, V.L., Feigl, A.B., Fereshtehnejad, S.-M., Fernandes, E., Fernandes, J.C., Ferrara, G., Ferrari, A.J., Ferreira, M.L., Filip, I., Finger, J.D., Fischer, F., Foigt, N.A., Foreman, K. J., Fukumoto, T., Fullman, N., FÃ¼rst, T., Furtado, J.O.M., Futran, N.D., Gall, S., Gallus, S., Gamkrelidze, A., Ganji, M., Garcia-Basteiro, A.L., Gardner, W.M., Gebre, A.K., Gebremedhin, A.T., Gebremichael, T.G., Gelano, T.F., Geleijnse, J.M., Geramo, Y.C.D., Gething, P.W., Gezae, K.E., Ghadimi, R., Ghadiri, K., Falavarjani, K. G., Ghasemi-Kasman, M., Ghimire, M., Ghosh, R., Ghoshal, A.G., Giampaoli, S., Gill, P.S., Gill, T.K., Gillum, R.F., Ginawi, I.A., Giussani, G., Gnedovskaya, E.V., Godwin, W.W., Goli, S., s, H.G.M.-D., Gona, P.N., Gopalani, S.V., Goulart, A.C., Grada, A., Grams, M.E., Grosso, G., Gugnani, H.C., Guo, Y., Gupta, R., Gupta, R., Gupta, T., rrez, R.A.G., rrez-Torres, D.S.G., Haagsma, J.A., Habtewold, T.D., Hachinski, V., Hafezi-Nejad, N., Hagos, T.B., Hailegiyorgis, T.T., Hailu, G.B., Haj-Mirzaian, A., Haj-Mirzaian, A., Hamadeh, R.R., Hamidi, S., Handal, A.J., Hankey, G. J., Hao, Y., Harb, H.L., Harikrishnan, S., Haro, J.M., Hassankhani, H., Hassen, H.Y., Havmoeller, R., Hawley, C.N., Hay, S.I., Hedayatizadeh-Omran, A., Heibati, B., Heidari, B., Heidari, M., Hendrie, D., Henok, A., Heredia-Pi, I., Herteliu, C., Heydarpour, F., Heydarpour, S., Hibstu, D.T., Higazi, T.B., Hilawe, E.H., Hoek, H.W., Hoffman, H.J., Hole, M.K., Rad, E.H., Hoogar, P., Hosgood, H.D., Hosseini, S.M., Hosseinzadeh, M., Hostiuc, M., Hostiuc, S., Hoy, D.G., Hsairi, M., Hsiao, T., Hu, G., Hu, H., Huang, J.J., Hussen, M.A., Huynh, C.K., Iburg, K.M., Ikeda, N., Ilesanmi, O. S., Iqbal, U., Irvani, S.S.N., Irvine, C.M.S., Islam, S.M.S., Islami, F., Jackson, M.D., Jacobsen, K.H., Jahangiry, L., Jahanmehr, N., Jain, S.K., Jakovljevic, M., James, S.L., Jassal, S.K., Jayatilleke, A.U., Jeemon, P., Jha, R.P., Jha, V., Ji, J.S., Jonas, J.B., Jonnagaddala, J., Shushtari, Z.J., Joshi, A., Jozwiak, J.J., JÃ¼risson, M., Kabir, Z., Kahsay, A., Kalani, R., Kanchan, T., Kant, S., Kar, C., Karami, M., Matin, B.K., Karch, A., Karema, C., Karimi, N., Karimi, S.M., Kasaeian, A., Kassa, D.H., Kassa, G. M., Kassa, T.D., Kassebaum, N.J., Katikireddi, S.V., Kaul, A., Kawakami, N., Kazemi, Z., Karyani, A.K., Kefale, A.T., Keiyoro, P.N., Kemp, G.R., Kengne, A.P., Keren, A., Kesavachandran, C.N., Khader, Y.S., Khafaei, B., Khafaie, M.A., Khajavi, A., Khalid, N., Khalil, I.A., Khan, G., Khan, M.S., Khan, M.A., Khang, Y.-H., Khater, M.M., Khazaei, M., Khazaie, H., Khoja, A.T., Khosravi, A., Khosravi, M.H., Kiadaliri, A.A., Kiirithio, D.N., Kim, C.-I., Kim, D., Kim, Y.-E., Kim, Y.J., Kimokoti, R. W., Kinfu, Y., Kisa, A., Kissimova-Skarbek, K., ki, M.K., Knibbs, L.D., Knudsen, A.K.S., Kochhar, S., Kokubo, Y., Kolola, T., Kopec, J.A., Kosen, S., Koul, P.A., Koyanagi, A., Kravchenko, M.A., Krishan, K., Krohn, K.J., Kromhout, H., Defo, B.K., Bicer, B.K., Kumar, G.A., Kumar, M., Kuzin, I., Kyu, H.H., Lachat, C., Lad, D.P., Lad, S.D., Lafranconi, A., Lalloo, R., Lallukka, T., Lami, F.H., Lang, J.J., Lansingh, Van C., Larson, S.L., Latifi, A., Lazarus, J.V., Lee, P.H., Leigh, J., Leili, M., Leshargie, C.T., Leung, J., Levi, M., Lewycka, S., Li, S., Li, Y., Liang, J., Liang, X., Liao, Y., Liben, M. L., Lim, L.-L., Linn, S., Liu, S., Lodha, R., Logroscino, G., Lopez, A.D., Lorkowski, S., Lotufo, P.A., Lozano, R., Lucas, T.C.D., Lunevicius, R., Ma, S., Macarayan, E.R.K., Machado, Ã.S.E., Madotto, F., Mai, H.T., Majdan, M., Majdzadeh, R., Majeed, A., Malekzadeh, R., Malta, D.C., Mamun, A.A., Manda, A.-L., Manguerra, H., Mansournia, M.A., Mantovani, L.G., Maravilla, J.C., Marcenes, W., Marks, A., Martin, R.V., Martins, S.C.O., Martins-Melo, F.R.N., rz, W.M., Marzan, M.B., Massenburg, B.B., Mathur, M.R., Mathur, P., Matsushita, K., Maulik, P.K., Mazidi, M., McAlinden, C., McGrath, J.J., McKee, M., Mehrotra, R., Mehta, K.M., Mehta, V., Meier, T., Mekonnen, F.A., Melaku, Y.A., Melese, A., Melku, M., Memiah, P.T.N., Memish, Z.A., Mendoza, W., Mengistu, D.T., Mensah, G.A., Mensink, G.B.M., Mereta, S.T., Meretoja, A., Meretoja, T.J., Mestrovic, T., Mezgebe, H.B., Miazgowski, B., Miazgowski, T., Millear, A.I., Miller, T.R., Miller-Petrie, M.K., Mini, G.K., Mirarefin, M., Mirica, A., Mirrakhimov, E.M., Misganaw, A. T., Mitiku, H., Moazen, B., Mohajer, B., Mohammad, K.A., Mohammadi, M., Mohammadifard, N., Mohammadnia-Afrouzi, M., Mohammed, S., Mohebi, F., Mokdad, A.H., Molokhia, M., Momeniha, F., Monasta, L., Moodley, Y., Moradi, G., Moradi-Lakeh, M., Moradinazar, M., Moraga, P., Morawska, L., Morgado-Da-Costa, J., Morrison, S.D., Moschos, M.M., Mouodi, S., Mousavi, S.M., Mozaffarian, D., Mruts, K.B., Muche, A.A., Muchie, K.F., Mueller, U.O., Muhammed, O.S., Mukhopadhyay, S., Muller, K., Musa, K.I., Mustafa, G., Nabhan, A. F., Naghavi, M., Naheed, A., Nahvijou, A., Naik, G., Naik, N., Najafi, F., Nangia, V., Nansseu, J.R., Nascimento, B.R., Neal, B., Neamati, N., Negoi, I., Negoi, R.I., Neupane, S., Newton, C.R.J., Ngunjiri, J.W., Nguyen, A.Q., Nguyen, G., Nguyen, H. T., Nguyen, H.L.T., Nguyen, H.T., Nguyen, M., Nguyen, N.B., Nichols, E., Nie, J., Ningrum, D.N.A., Nirayo, Y.L., Nishi, N., Nixon, M.R., Nojomi, M., Nomura, S., Norheim, O.F., Noroozi, M., Norrving, B., Noubiap, J.J., Nouri, H.R., Shiadeh, M.N., Nowroozi, M.R., Nsoesie, E.O., Nyasulu, P.S., Obermeyer, C.M., Odell, C.M., Ofori-Asenso, R., Ogbo, F.A., Oh, I.-H., Oladimeji, O., Olagunju, A.T., Olagunju, T.O., Olivares, P.R., Olsen, H.E., Olusanya, B.O., Olusanya, J.O., Ong, K.L., Ong, S.K., Oren, E., Orpana, H.M., Ortiz, A., Ota, E., Otstavnov, S.S., verland, S.Ã., Owolabi, M. O., P A M, Pacella, R., Pakhare, A.P., Pakpour, A.H., Pana, A., Panda-Jonas, S., Park, E.-K., Parry, C.D.H., Parsian, H., Patel, S., Pati, S., Patil, S.T., Patle, A., Patton, G.C., Paudel, D., Paulson, K.R., Ballesteros, W.C.P., Pearce, N., Pereira, A., Pereira, D.M., Perico, N., Pesudovs, K., Petzold, M., Pham, H.Q., Phillips, M.R., Pillay, J.D., Piradov, M.A., Pirsaheb, M., Pischon, T., Pishgar, F., Plana-Ripoll, O., Plass, D., Polinder, S., Polkinghorne, K.R., Postma, M.J., Poulton, R., Pourshams, A., Poustchi, H., Prabhakaran, D., Prakash, S., Prasad, N., Purcell, C.A., Purwar, M.B., Qorbani, M., Radfar, A., Rafay, A., Rafiei, A., Rahim, F., Rahimi, Z., Rahimi-Movaghar, A., Rahimi-Movaghar, V., Rahman, M., Rahman, M.H.U., Rahman, M.A., Rai, R.K., Rajati, F., Rajsic, S., Raju, S.B., Ram, U., Ranabhat, C.L., Ranjan, P., Rath, G.K., Rawaf, D.L., Rawaf, S., Reddy, K.S., Rehm, C.D., Rehm, J., Reiner Jr., R. C., Reitsma, M.B., Remuzzi, G., Renzaho, A.M.N., Resnikoff, S., Reynales-Shigematsu, L.M., Rezaei, S., Ribeiro, A.L.P., Rivera, J.A., Roba, K.T., rez, S.R.G.-R., Roever, L., n, Y.R., Ronfani, L., Roshandel, G., Rostami, A., Roth, G.A., Rothenbacher, D., Roy, A., Rubagotti, E., Rushton, L., Sabanayagam, C., Sachdev, P. S., Saddik, B., Sadeghi, E., Moghaddam, S.S., Safari, H., Safari, Y., Safari-Faramani, R., Safdarian, M., Safi, S., Safiri, S., Sagar, R., Sahebkar, A., Sahraian, M. A., Sajadi, H.S., Salam, N., Salamati, P., Saleem, Z., Salimi, Y., Salimzadeh, H., Salomon, J.A., Salvi, D.D., Salz, I., Samy, A.M., Sanabria, J., o, M.D.S.-N., nchez-Pimienta, T.G.S., Sanders, T., Sang, Y., Santomauro, D.F., Santos, I.S., Santos, J.O.V., Milicevic, M.M.S., Jose, B.P.S., Sardana, M., Sarker, A.R., rez, R.S.-S., Sarrafzadegan, N., Sartorius, B., Sarvi, S., Sathian, B., Satpathy, M., Sawant, A.R., Sawhney, M., Saylan, M., Sayyah, M., Schaeffner, E., Schmidt, M.I., Schneider, I.J.C., SchÃ ttker, Ben, Schutte, A.E., Schwebel, D.C., Schwendicke, F., Scott, J.G., Seedat, S., Sekerija, M., Sepanlou, S.G., Serre, M.L., n-Mori, E.S., Seyedmousavi, S., Shabaninejad, H., Shaddick, G., Shafieesabet, A., Shahbazi, M., Shaheen, A.A., Shaikh, M.A., Levy, T.S., Shams-Beyranvand, M., Shamsi, M., Sharafi, H., Sharafi, K., Sharif, M., Sharif-Alhoseini, M., Sharifi, H., Sharma, J., Sharma, M., Sharma, R., She, J., Sheikh, A., Shi, P., Shibuya, K., Shiferaw, M.S., Shigematsu, M., Shin, M.-J., Shiri, R., Shirkoohi, R., Shiue, I., Shokraneh, F., Shoman, H., Shrime, M.G., Shupler, M.S., Si, S., Siabani, S., Sibai, A.M., Siddiqi, T.J., Sigfusdottir, I.D., Sigurvinsdottir, R., Silva, D.A.S., Silva, J.O.P., Silveira, D.G.A., Singh, J.A., Singh, N. P., Singh, V., Sinha, D.N., Skiadaresi, E., Skirbekk, V., Smith, D.L., Smith, M., Sobaih, B.H., Sobhani, S., Somayaji, R., Soofi, M., Sorensen, R.J.D., Soriano, J.B., Soyiri, I.N., Spinelli, A., Sposato, L.A., Sreeramareddy, C.T., Srinivasan, V., Starodubov, V.I., Steckling, N., Stein, D.J., Stein, M.B., Stevanovic, G., Stockfelt, L., Stokes, M.A., Sturua, L., Subart, M.L., Sudaryanto, A., Sufiyan, M.B., Sulo, G., Sunguya, B.F., Sur, P.J., Sykes, B.L., Szoeke, C.E.I., s-Seisdedos, R.T., Tabuchi, T., Tadakamadla, S.K., Takahashi, K., Tandon, N., Tassew, S.G., Tavakkoli, M., Taveira, N., Tehrani-Banihashemi, A., Tekalign, T.G., Tekelemedhin, S.W., Tekle, M. G., Temesgen, H., Temsah, M.-H., Temsah, O., Terkawi, A.S., Tessema, B., Teweldemedhin, M., Thankappan, K.R., Theis, A., Thirunavukkarasu, S., Thomas, H. J., Thomas, M.L., Thomas, N., Thurston, G.D., Tilahun, B., Tillmann, T., To, Q.G., Tobollik, M., Tonelli, M., Topor-Madry, R., Torre, A.E., s, M.T.-G., Touvier, M., Tovani-Palone, M.R., Towbin, J.A., Tran, B.X., Tran, K.B., Truelsen, T.C., Truong, N. T., Tsadik, A.G., Car, L.T., Tuzcu, E.M., Tymeson, H.D., Tyrovolas, S., Ukwaja, K.N., Ullah, I., Updike, R.L., Usman, M.S., Uthman, O.A., Vaduganathan, M., Vaezi, A., Valdez, P.R., van Donkelaar, A., Varavikova, E., Varughese, S., Vasankari, T.J., Venkateswaran, V., Venketasubramanian, N., Villafaina, S., Violante, F.S., Vladimirov, S.K., Vlassov, V., Vollset, S.E., Vos, T., Vosoughi, K., Vu, G.T., Vujcic, I. S., Wagnew, F.S., Waheed, Y., Waller, S.G., Walson, J.L., Wang, Y., Wang, Y., Wang, Y.-P., Weiderpass, E., Weintraub, R.G., Weldegebreal, F., Werdecker, A., Werkneh, A.A., West, J.J., Westerman, R., Whiteford, H.A., Widecka, J., Wijeratne, T., Winkler, A.S., Wiyeh, A.B., Wiysonge, C.S., Wolfe, C.D.A., Wong, T.Y., Wu, S., Xavier, D., Xu, G., Yadgir, S., Yadollahpour, A., Jabbari, S.H.Y., Yamada, T., Yan, L.L., Yano, Y., Yaseri, M., Yasin, Y.J., Yeshaneh, A., Yimer, E.M., Yip, P., Yisma, E., Yonemoto, N., Yoon, S.-J., Yotebieng, M., Younis, M.Z., Yousefifard, M., Yu, C., Zaidi, Z., Bin Zaman, S., Zamani, M., Zavala-Arciniega, L., Zhang, A.L., Zhang, H., Zhang, K., Zhou, M., Zimsen, S.R.M., Zodpey, S., Murray, C.J.L., Collaborators, G.2.R.F, 2018. Global, Regional, and national comparative risk assessment of 84 behavioural, environmental and occupational, and metabolic risks or clusters of risks for 195 countries and territories, 1990-2017: a systematic analysis for the global burden of disease study 2017. Lancet 392 (10159), 1923–1994.

Still, D., Bentson, S., Li, H., 2015. Results of laboratory testing of 15 cookstove designs in accordance with the ISO/IWA tiers of performance. EcoHealth 12, 12–24.

Sutar, K.B., Kohli, S., Ravi, M.R., Ray, A., 2015. Biomass cookstoves: a review of technical aspects. Renew. Sustain. Energy Rev. 41, 1128–1166.

Taylor, J.R., 1997. An Introduction to Error Analysis: the Study of Uncertainties in Physical Measurements. University Science Books, Sausalito, CA, pp. 1–1.

The Water Boiling Test, 4 ed., 2014. Global Alliance for Clean Cookstoves, pp. 1–89.

Tissari, J., Lyyränen, J., Hytönen, K., Sippula, O., Tapper, U., Frey, A., Saarnio, K., Pennanen, A.S., Hillamo, R., Salonen, R.O., Hirvonen, M.R., Jokiniemi, J., 2008. Fine particle and gaseous emissions from normal and smouldering wood combustion in a conventional masonry heater. Atmos. Environ. 42 (34), 7862–7873.

Torvela, T., Tissari, J., Sippula, O., Kaivosoja, T., Leskinen, J., Virén, A., Lähde, A., Jokiniemi, J., 2014. Effect of wood combustion conditions on the morphology of freshly emitted fine particles. Atmos. Environ. 87, 65–76.

Tryner, J., Tillotson, J.W., Baumgardner, M.E., Mohr, J.T., DeFoort, M.W., Marchese, A. J., 2016. The effects of air flow rates, secondary air inlet geometry, fuel type, and operating mode on the performance of gasifier cookstoves. Environ. Sci. Technol. 50 (17), 9754–9763.

Valavanidis, A., Fiotakis, K., Vlachogianni, T., 2008. Airborne particulate matter and human health: toxicological assessment and importance of size and composition of particles for oxidative damage and carcinogenic mechanisms. Journal of Environmental Science and Health, Part C 26 (4), 339–362.

Vicente, E.D., Alves, C.A., 2018. An overview of particulate emissions from residential biomass combustion. Atmos. Res. 199, 159–185.

Wang, Y., Sohn, M.D., Wang, Y., Lask, K.M., Kirchstetter, T.W., Gadgil, A.J., 2014. How many replicate tests are needed to test cookstove performance and emissions? — three is not always adequate. Energy for Sustainable Development 20, 21–29.

Wiinikka, H., Gebart, R., 2004. Critical parameters for particle emissions in small-scale fixed-bed combustion of wood pellets. Energy Fuels 18 (4), 897–907.

Wiinikka, H., Gebart, R., 2005. The influence of air distribution rate on particle emissions in fixed bed combustion of biomass. Combust. Sci. Technol. 177 (9), 1747–1766.